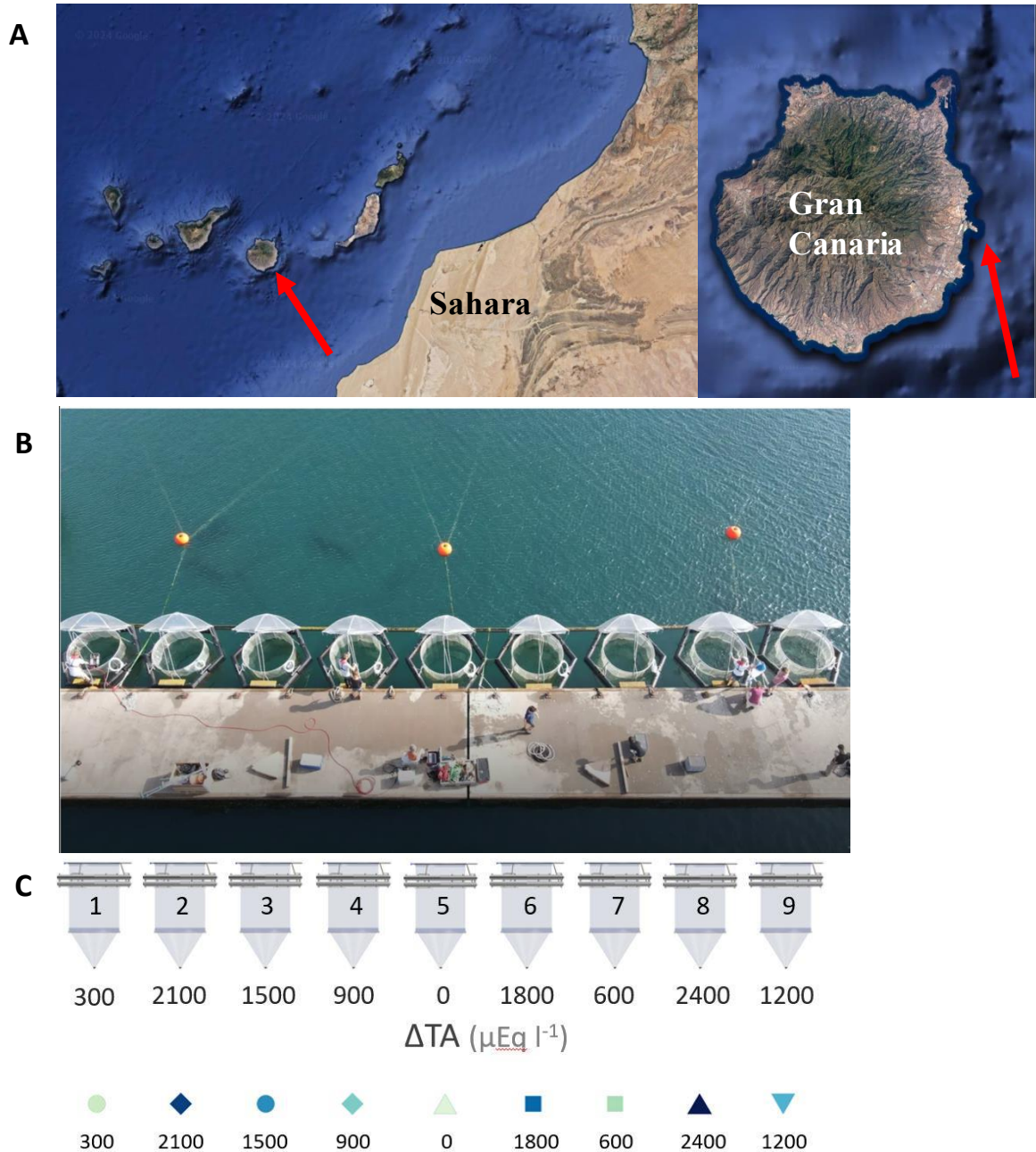


### Supplementary material

#### **Ocean Alkalinity Enhancement does not cause cellular stress in phytoplankton in a mesocosm experiment.**

Librada Ramírez <sup>1\*</sup>, Leonardo J. Pozzo-Pirotta <sup>1</sup>, Aja Trebec <sup>2</sup>, Víctor Manzanares-Vázquez <sup>1</sup>, José L. Díez <sup>1</sup>, Javier Arístegui <sup>2</sup>, Ulf Riebesell <sup>3</sup>, Stephen D. Archer <sup>4</sup>, María Segovia <sup>1</sup>.

\*Corresponding author: [librada@uma.es](mailto:librada@uma.es)



**Figure S1.** A) Study site in the port of Taliarte, Gran Canaria (Spain). B) Operating mesocosms during the experiment (photograph by Peter Yeung, National Geographic ©). C) Mesocosms experimental design representing the alkalinity gradient (OAE) ( $\mu\text{mol}\cdot\text{L}^{-1}$ ) in the nine mesocosms: M5 (0), M1 (300), M7 (600), M4 (900), M9 (1200), M3 (1500), M6 (1800), M2 (2100), M8 (2400) (design by Silvan Goldenberg ©, GEOMAR).

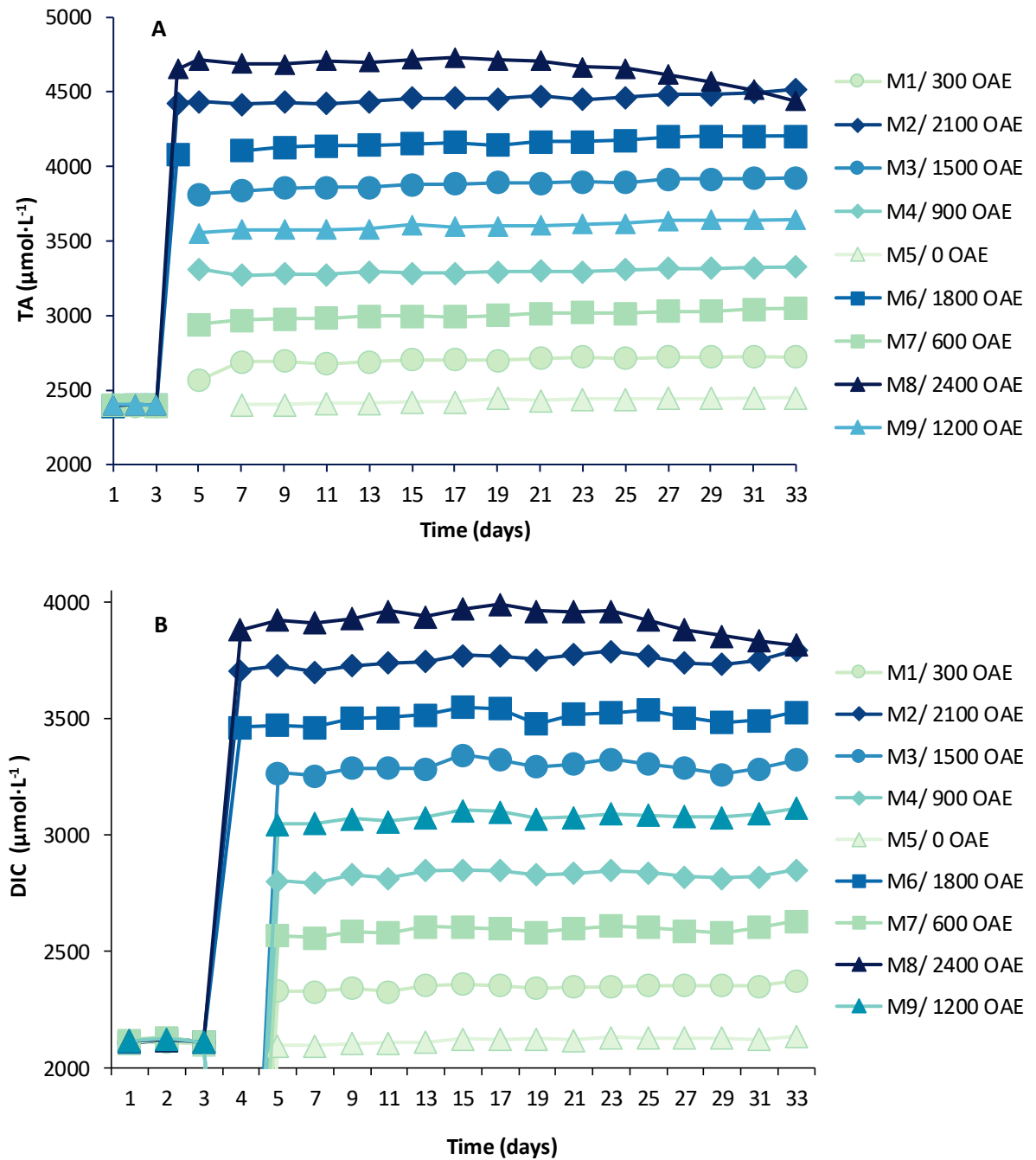
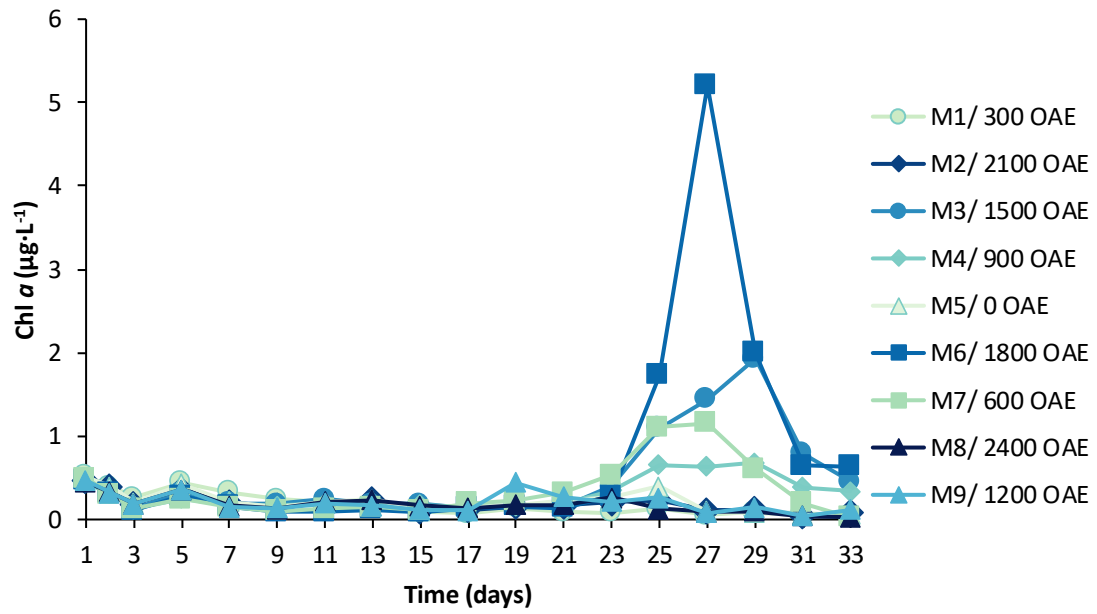
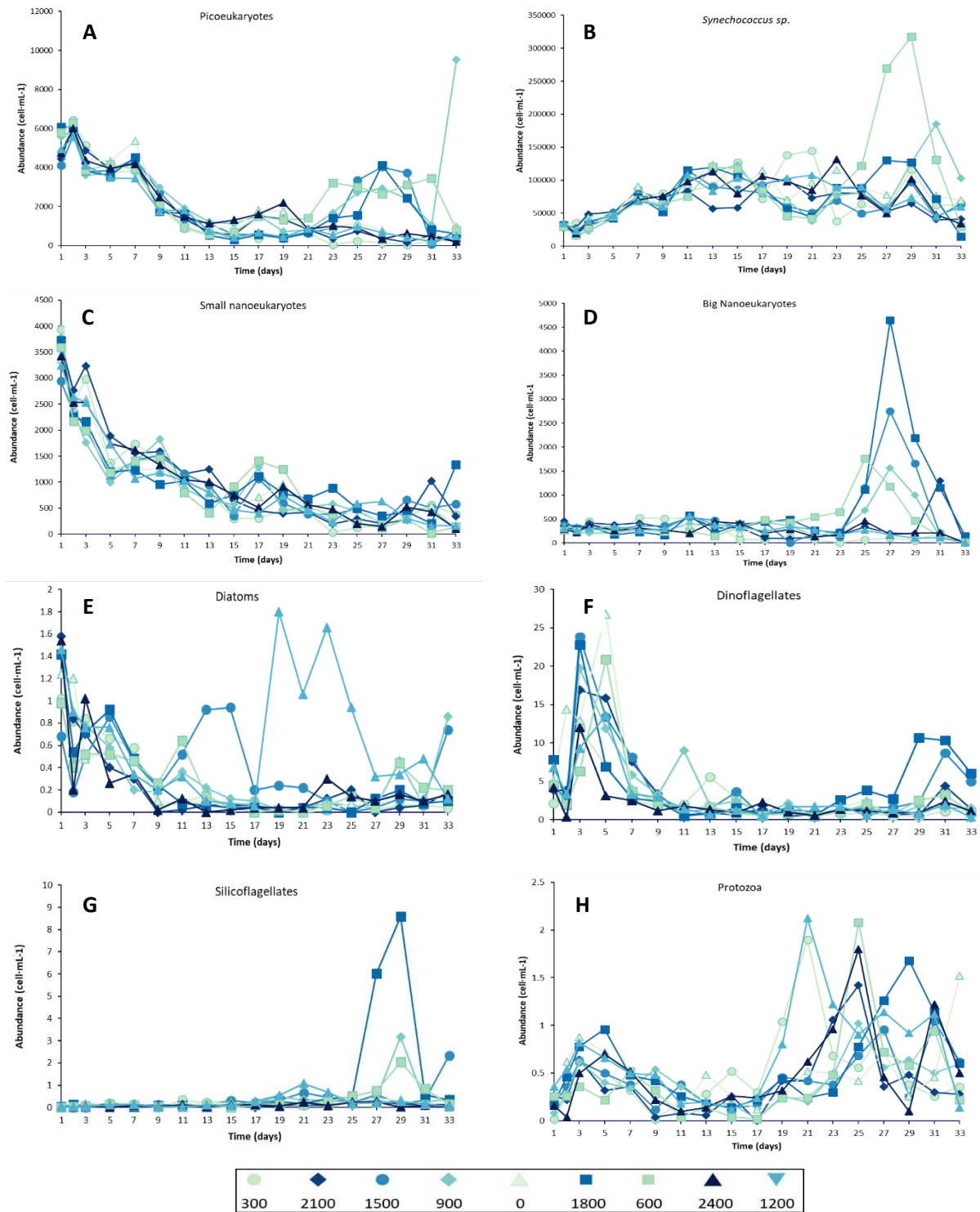


**Figure S2.** A) Evolution of total alkalinity (TA) ( $\mu\text{mol}\cdot\text{L}^{-1}$ ); and B) dissolved inorganic carbon (DIC) ( $\mu\text{mol}\cdot\text{L}^{-1}$ ) over time during the mesocosms experiment. Reproduction with permission of *Biogeosciences*, Marin-Samper et al. 2024.



**FigureS3.** Temporal evolution of chlorophyll-*a* concentration in  $\mu\text{g}\cdot\text{L}^{-1}$  during the mesocosms experiment. Reproduction with permission of *Biogeosciences*, Marin -Samper *et al.* 2024.



**FigureS4.** Cell abundance of phyto- and microphytoplankton in cell·mL<sup>-1</sup>. A) Picoeukaryotes <2  $\mu$ m; B) *Synechococcus* spp. < 2  $\mu$ m; C) Small nanoeukaryotes 2-20  $\mu$ m; D) Large nanoeukaryotes >20  $\mu$ m; E) Diatoms; F) Dinoflagellates; G) Silicoflagellates; H) Protozoa. Reproduction in with permission of *Biogeosciences*, *Marin -Samper et al. 2024 for A to D.*

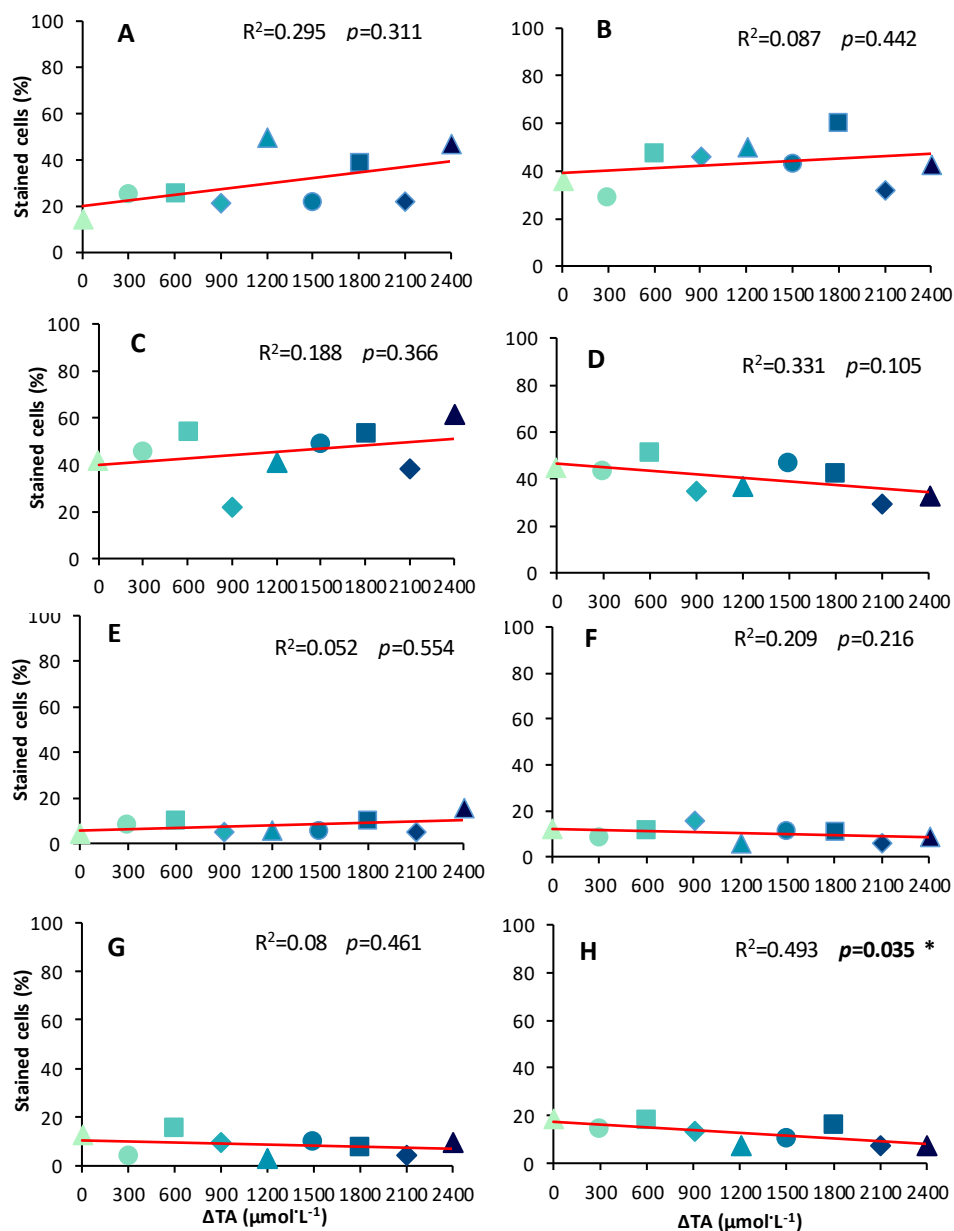


**Figure S5.** Linear regressions among the percentage of stained cells and OAE treatments in picoeukaryotes and *Synechococcus* spp. A) Cell viability (FDA) in picoeukaryotes in phase I; B) Cell viability in picoeukaryotes in phase II; C) Oxidative stress (ROS) in picoeukaryotes in phase I; D) Oxidative stress in picoeukaryotes in phase II; E) Cell viability in *Synechococcus* in phase I; F) Cell viability in *Synechococcus* in phase II; G) Oxidative stress in *Synechococcus* in phase I; H) Oxidative stress in *Synechococcus* in phase II.

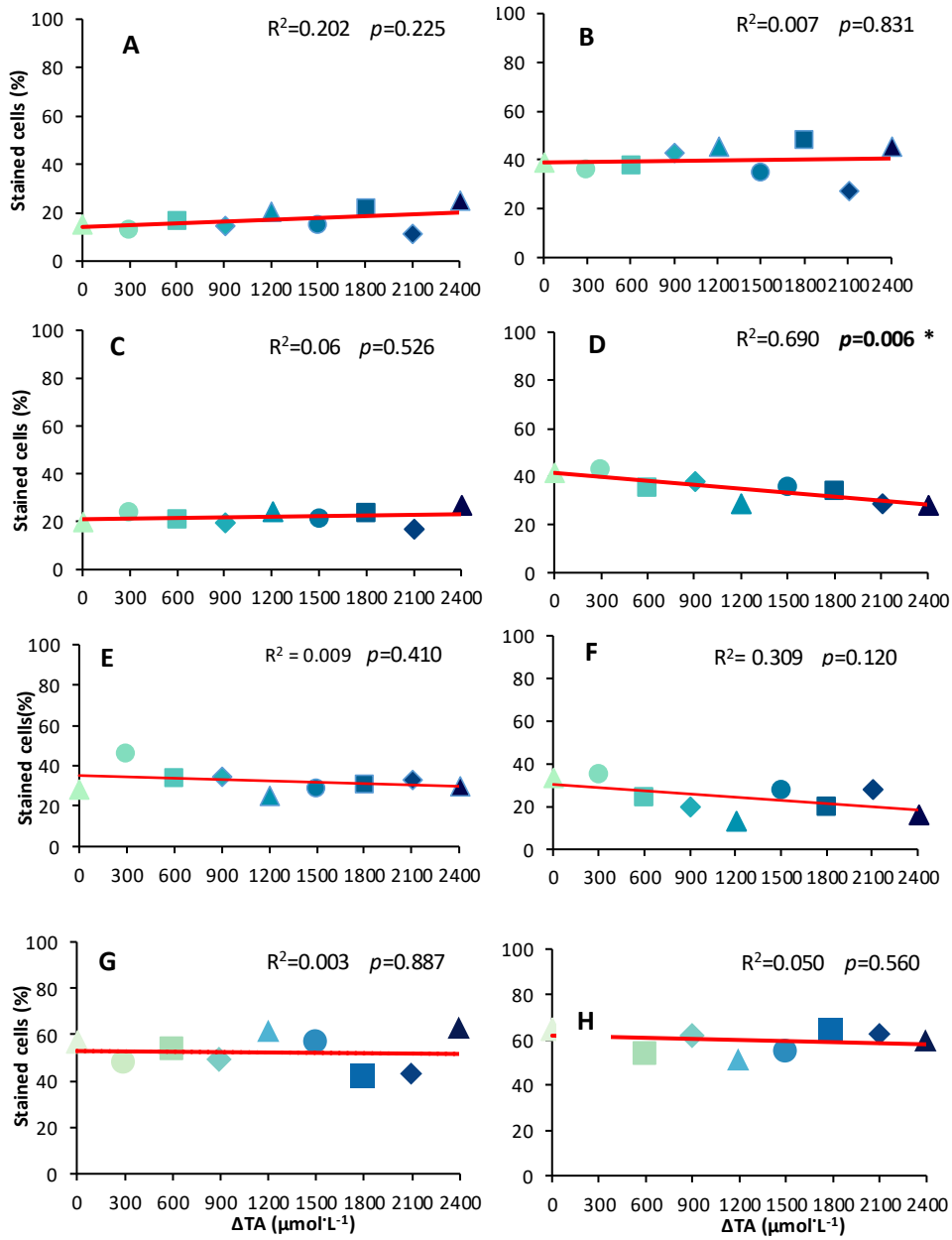
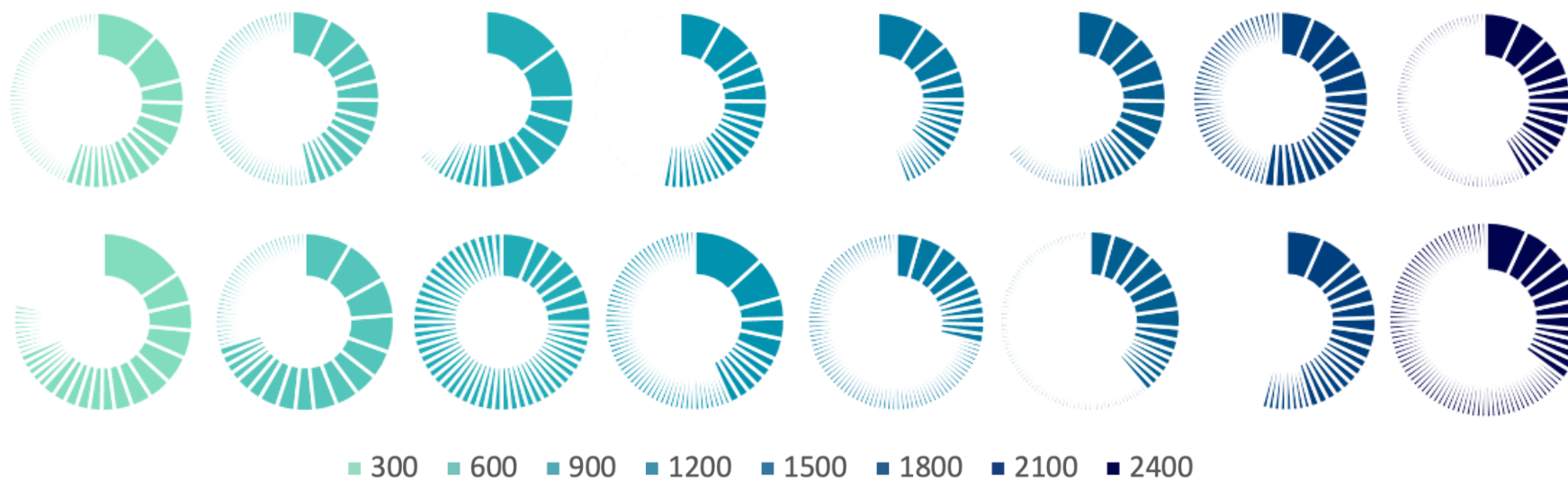


**Figure S6.** Linear regressions among the percentage of stained cells and OAE treatments in small nanoeukaryotes (20  $\mu\text{m}$ ) and big nanoeukaryotes (>20  $\mu\text{m}$ ). A) Cell viability (FDA) in small nanoeukaryotes in phase I; B) Cell viability in small nanoeukaryotes in phase II; C) Oxidative stress (ROS) in small nanoeukaryotes in phase I; D) Oxidative stress in small nanoeukaryotes in phase II; E) Cell viability in big nanoeukaryotes in phase II; F) Oxidative stress in big nanoeukaryotes in phase II; G) Cell viability in microphytoplankton in phase II; H) Oxidative stress in microphytoplankton in phase II.

Upregulated  
protein  
abundances

Downregulated  
protein  
abundances



$\Delta\text{TA } \mu\text{mol} \cdot \text{L}^{-1}$

**Figure S7.** Ring-Sector plots categorized by absolute abundances of significantly upregulated and downregulated protein abundances normalised to  $\Delta\text{TA } 0 \mu\text{mol} \cdot \text{L}^{-1}$  and housekeeping proteins. By ring-around each sector, the protein that has changed its abundance will appear, attending to its contribution amongst all the up/down-regulated dataset.

